

Tidal resonance in extreme mass-ratio inspirals

Béatrice Bonga,¹ Huan Yang,^{1,2} and Scott A. Hughes³

¹*Perimeter Institute for Theoretical Physics, Waterloo, Ontario N2L 2Y5, Canada*

²*University of Guelph, Guelph, Ontario N2L 3G1, Canada*

³*Department of Physics and Kavli Institute for Astrophysics and Space Research, Massachusetts Institute of Technology, Cambridge, Massachusetts 02139, USA*

We describe a new class of resonances for extreme mass-ratio inspirals (EMRIs): tidal resonances, induced by the tidal field of nearby stars or stellar-mass black holes. A tidal resonance can be viewed as a general relativistic extension of the Kozai-Lidov resonances in Newtonian systems, and is distinct from the transient resonance already known for EMRI systems. Tidal resonances will generically occur for EMRIs. By probing their influence on the phase of an EMRI waveform, we can learn about the tidal environment of the EMRI system, albeit at the cost of a more complicated waveform model. Observations by LISA of EMRI systems therefore have the potential to provide information about the distribution of stellar-mass objects near their host galactic-center black holes.

Introduction. Ground-based gravitational-wave (GW) detectors have achieved tremendous success observing merging stellar-mass black holes (BHs) and neutron stars. At lower frequencies (\sim mHz), the Laser Interferometer Space Antenna (LISA) will probe binaries involving massive BHs at the centers of galaxies[1].

One important source class for LISA are extreme mass-ratio inspirals (EMRIs), stellar-mass objects (typically a $10\text{--}30 M_\odot$ BH) spiraling into a massive ($\sim 10^5\text{--}10^7 M_\odot$) BH in a galactic center. The large separation of mass scales means that the stellar-mass object's influence on the binary may be approximated as a perturbation of the large BH's spacetime. These stellar-mass objects typically undergo $10^5\text{--}10^6$ orbits near the large BH in the LISA frequency band before finally plunging, providing a unique laboratory for mapping the spacetimes of BHs and enabling precise tests of strong-field gravity (see, for example, [2] for a recent review).

In this *Letter*, we propose that GW observations of EMRIs can be used to probe the environmental tidal field generated by stars and BHs near an EMRI system. The EMRI waveforms will encode information about the BH and stellar distribution in galactic centers which are difficult to obtain with electromagnetic observations. We show that an environmental tidal field introduces a new type of resonance behavior, hereafter called *tidal resonance*, on the EMRI waveform. This effect can be intuitively understood as the general relativistic extension of the Newtonian Kozai-Lidov resonance [3]. Tidal resonances are different from transient resonances [4], which arise from the gravitational self-force.

BHs near EMRIs. Galactic centers are crowded environments. There are good theoretical reasons to expect several $10^5 M_\odot$ in stellar-mass BHs inside the inner parsec around a galaxy's central BH [5, 6] and there is (tentative) observational evidence supporting this for our own galaxy [7]. Scattering processes can put stellar-mass objects (such as stars and black holes) near enough to the massive BHs in galactic centers for the object to be gravitationally bound to the BH. Mean-motion resonance, in

which a pair of stellar-mass objects jointly migrates towards the massive black hole until the resonant locking breaks down [8], can also bring BHs close to the massive BH.

Currently, the distribution of stellar-mass objects nearby massive BHs is not well known. Proper dynamical theory calculations or N -body simulations are needed to compute the distribution of stellar-mass objects near galactic center BHs and assess the distance of the outliers closest to the central BH. Predictions based on a Fokker-Planck simulation suggest that a population of $40 M_\odot$ BHs can be close to Sagittarius A*, with median distance ~ 5 AU [9, 10]. This is roughly consistent with the following simple estimate for the distance of the closest BH, which mimics an argument in [11]. The EMRI merger rate is about [12]

$$\frac{1}{T_{\text{EMRI}}} \approx 0.3 \left(\frac{M}{10^6 M_\odot} \right)^{0.19} \text{Myr}^{-1}, \quad (1)$$

where T_{EMRI} is the interval between EMRI events, and M is the mass of the central BH. Note that this estimate is subject to significant model uncertainties. Assuming that orbit decay is mainly driven by GW emission, at the time of an EMRI the distance R to the next infalling BH (with mass M_\star) can be estimated using

$$T_{\text{EMRI}} \sim \frac{R}{\dot{R}} \sim \frac{5}{64} \frac{c^5 R^4}{G^3 M_\star M^2}, \quad (2)$$

telling us that

$$R \sim 4.3 \text{ AU} \left(\frac{M_\star}{10 M_\odot} \right)^{1/4} \left(\frac{M}{M_{\text{SgrA}^*}} \right)^{0.45}, \quad (3)$$

with $M_{\text{SgrA}^*} = 4 \times 10^6 M_\odot$ the mass of Sagittarius A*.

Although it is interesting that this estimate agrees with [9, 10], we emphasize that it is only meant to provide a plausible case that a stellar mass black hole can be close enough for its tides to significantly influence an EMRI's orbital evolution. In particular, this estimate ignores the

fact that the tidal perturber's orbit will surely be eccentric. A critical point is that, because the tidal field scales as M_\star/R^3 , the nearest outliers from a distribution of stellar mass black holes in the innermost regions of a galaxy (such as discussed in [5–7]) will have the strongest impact, significantly greater than the tides from another massive BH at ~ 0.1 pc (considered in [13]). The closest stellar-mass BHs are likely to be the main contributors to the tidal environment of EMRIs.

Tidal resonance. An EMRI orbit deviates from BH geodesic motion due to the gravitational self-force [14] and the tidal field from nearby stars and BHs. The induced acceleration by the tidal field is generally smaller than that of the self-force. As we are interested in the EMRI motion near the central massive BH, it is natural to apply BH perturbation techniques [14] instead of post-Newtonian simulations as was done in [11].

There is a two-timescale separation in the description of EMRI orbital evolution [15]. This separation simplifies the analysis, approximating the orbit at any moment as a geodesic (with evolving integrals of motion) plus perturbations. The fast timescale corresponds to the cyclic motion, and the slow timescale to the secular change of conserved quantities by radiation reaction. As Kerr geodesic motion is separable [16], it is convenient to use action-angle variables $q_{r,\theta,\phi}$ to describe the motion in (r, θ, ϕ) :

$$\begin{aligned} \frac{dq_i}{d\tau} &= \omega_i(\mathbf{J}) + \epsilon g_{i,\text{td}}^{(1)}(q_\phi, q_\theta, q_r, \mathbf{J}) + \eta g_{i,\text{sf}}^{(1)}(q_\theta, q_r, \mathbf{J}) \\ &\quad + \mathcal{O}(\eta^2, \epsilon^2, \eta\epsilon), \\ \frac{dJ_i}{d\tau} &= \epsilon G_{i,\text{td}}^{(1)}(q_\phi, q_\theta, q_r, \mathbf{J}) + \eta G_{i,\text{sf}}^{(1)}(q_\theta, q_r, \mathbf{J}) \\ &\quad + \mathcal{O}(\eta^2, \epsilon^2, \eta\epsilon). \end{aligned} \quad (4)$$

The action variables $\mathbf{J} := \{J_r, J_\theta, J_\phi\}$ are functions of the energy E , angular momentum along the symmetry axis L_z and the Carter constant Q ; η is the EMRI mass ratio, and $\epsilon := M_\star M^2/R^3$ characterizes the strength of the tidal field produced by the third body M_\star . The parameter τ is the proper time of the inspiraling body. The terms $G_i^{(1)}$ and $g_i^{(1)}$ force the orbit away from geodesic motion. Terms with subscript “td” are from the tidal force, and depend upon the axial angle ϕ and the third body M_\star ; terms with subscript “sf” are from the self-force (generated by gravitational radiation reaction) and do not depend on ϕ and M_\star . Without the self-force and the tidal force, \mathbf{J} would be conserved quantities and q_i would increase at a fixed rate in time.

Focus now on the tidal force $G_{i,\text{td}}^{(1)}$ and drop the subscript “td.” We write this term in the frequency domain

$$G_i^{(1)}(q_\phi, q_\theta, q_r, \mathbf{J}) = \sum_{m,k,n} G_{i,mkn}^{(1)}(\mathbf{J}) e^{i(mq_\phi + kq_\theta + nq_r)}, \quad (5)$$

with m, k, n integer. Over the total duration of the EMRI inspiral ($\propto M/\eta$), the dissipative part of the self-

force ($\propto \eta$) changes the conserved quantities by a fractional amount of order unity. In $G_i^{(1)}$, the exponential in $q_{\phi,\theta,r}$ generally oscillates in time, so a typical mode with nonzero m, k, n will vanish after orbit averaging, and consequently does not contribute to secular changes of conserved quantities. However, in special cases one can have

$$\omega_{mkn} := m\omega_\phi + k\omega_\theta + n\omega_r = 0, \quad (6)$$

so that the exponential does not oscillate. If the corresponding force amplitude $G_{i,mkn}$ is non-zero, this mode will induce a secular change in \mathbf{J} . This is the tidal resonance. By Eq. (4), both \mathbf{J} and $\omega_i(\mathbf{J})$ change at the radiation reaction timescale M/η . The tidal resonance is thus transient because of the orbit's inspiral. However, it occurs under more general conditions than the transient resonance of the gravitational self-force [4], which requires $k\omega_\theta + n\omega_r = 0$. Transient resonances have been shown to occur for generic EMRIs [17, 18]; the same conclusion should apply for tidal resonances since its resonance condition is more general. Moreover, tidal resonances will exist for low eccentricity orbits, whereas the transient resonance may be unimportant for many LISA EMRI sources due to low eccentricity [19].

The tidal resonance induces a change in \mathbf{J} . Defining $\tau = 0$ as the moment of resonance, and expanding q_i around this point as $q_{i0} + \omega_{i0}\tau + \dot{\omega}_{i0}\tau^2 + \mathcal{O}(\tau^3)$, this change across the resonance is well-approximated by [4]

$$\begin{aligned} \Delta J_i &= \epsilon \int_{-\infty}^{\infty} G_i^{(1)}(q_\phi, q_\theta, q_r, \mathbf{J}) d\tau \\ &= \frac{\epsilon}{\eta^{1/2}} \sum_s \sqrt{\frac{2\pi}{|\Gamma s|}} \exp\left[\text{sgn}(\Gamma s) \frac{i\pi}{4} + is\chi\right] G_{i,sm\ sk\ sn}^{(1)}, \end{aligned} \quad (7)$$

with $\chi := mq_{\phi 0} + kq_{\theta 0} + nq_{r 0}$, s a non-zero integer, and $\Gamma := m\dot{\omega}_{\phi 0} + k\dot{\omega}_{\theta 0} + n\dot{\omega}_{r 0}$; terms with $s = \pm 1$ dominate. All quantities are evaluated at resonance. As $\Delta \mathbf{J}$ is proportional to $\epsilon/\eta^{1/2}$, the accumulated phase shift over $1/\eta$ inspiral cycles is proportional to $\epsilon/\eta^{3/2}$.

In Eq. (7), we ignore changes of the external tidal field during the resonance. This is valid if the orbital period of the perturbing third body, $T_{\text{td}} \sim 2\pi\sqrt{R^3/M}$, is much longer than the resonance's duration, $T_{\text{res}} \sim 1/\sqrt{\eta\Gamma}$. When this holds, the tidal field is effectively static during the resonance. It is possible that the third body is so close to the EMRI that $T_{\text{td}} \lesssim T_{\text{res}}$. In such a case, if the third body's orbit is near the EMRI's equatorial plane and has azimuthal frequency Ω_ϕ , we only need to correct $q_{\phi 0}$: the tidal resonance is shifted to $m(\omega_\phi \mp \Omega_\phi) + k\omega_\theta + n\omega_r = 0$ (upper sign for prograde motion of the third body, lower for retrograde). Because $\Omega_\phi \ll \omega_\phi$, such a resonance is dynamically the same as in the $T_{\text{td}} \gg T_{\text{res}}$ case, but is evaluated at a slightly different frequency. In the most general setting, G_i must include the motion of the third body or the time dependence of the tidal field in Eq. (7).

To evaluate G_i , we need the perturbation $h_{\alpha\beta}$ to the central BH's spacetime due to the tidal field. This is found by solving Teukolsky's equation [20] in the slow motion limit followed by metric reconstruction [21]. For simplicity, we put the tidal perturber on the $(x-y)$ equatorial plane and only consider its quadrupolar nature (the dipolar perturbations induced are zero), with the massive BH spin along the z -axis [33]. As we will see, this restricts the type of resonances encountered. Specifically, we choose as the tidal moment tensor $\mathcal{E}_{ab} = (M_*/R^3)(2\nabla_a x \nabla_b x - \nabla_a y \nabla_b y - \nabla_a z \nabla_b z)$, where x , y , and z describe the motion of the perturbing third body in Cartesian-like coordinates (see Sec. IX B of [22]). We substitute this in Eqs. (7), (45), and (46) of [21] to obtain $h_{\alpha\beta}$ in the ingoing radiation gauge in advanced Eddington-Finkelstein coordinates [34]. Next, we perform a co-ordinate transformation to Boyer-Lindquist coordinates. Given $h_{\alpha\beta}$, we can compute the induced acceleration with respect to the background Kerr spacetime

$$a^\alpha = -\frac{1}{2}(g_{\text{Kerr}}^{\alpha\beta} + u^\alpha u^\beta)(2h_{\beta\lambda;\rho} - h_{\lambda\rho;\beta})u^\lambda u^\rho, \quad (8)$$

with u^α the unit vector tangent to the worldline of the EMRI's small mass μ . The corresponding instantaneous change rates of the integrals of motion are [13]

$$\frac{dL_z}{d\tau} = a_\phi \quad (9)$$

$$\frac{dQ}{d\tau} = 2u_\theta a_\theta - 2a^2 \cos^2 \theta u_t a_t + 2 \cot^2 \theta u_\phi a_\phi. \quad (10)$$

The energy E is conserved as the spacetime is assumed to be stationary during the resonance.

Sample evolutions. To illustrate the tidal resonance and to estimate its impact on the phase of an EMRI waveform, we consider three different scenarios summarized in Tab. I and Fig. 1. In all these scenarios, the EMRI crosses a tidal resonance with $m : k : n = -2 : 2 : 1$ [35].

After orbit averaging, the sum in Eq. (5) is

$$\langle G_i^{(1)}(q_\phi, q_\theta, q_r, \mathbf{J}) \rangle \approx G_{i,-2,2,1}^{(1)}(\mathbf{J}) e^{-2iq_\phi} + \text{cc}. \quad (11)$$

With $G_{i,-2,2,1}^{(1)}$, we compute $\Delta Q, \Delta L_z$ as a function of χ using Eq. (7). For this, we also need Γ , which we calculate

TABLE I: Three prograde orbital motions. Fig. 1 shows the dependence on $q_{\phi 0}$, which has the same functional form for all three cases.

a^a	r_{\min}	r_{\max}	θ_{\min}^b	$\dot{Q}_{-2,2,1}$	$\dot{L}_{-2,2,1}$
0.7	3.5	5.1628033	$\pi/3$	$1.66 + 2.27i$	$-0.35 - 0.47i$
0.9	3	6.6159726	$\pi/4$	$6.60 + 7.70i$	$-1.72 - 2.01i$
0.99	3	5.3718120	$\pi/4$	$4.46 + 3.43i$	$-1.23 - 0.95i$

^aDimensionless spin of the central BH.

^b $\theta_{\min} = \pi - \theta_{\max}$.

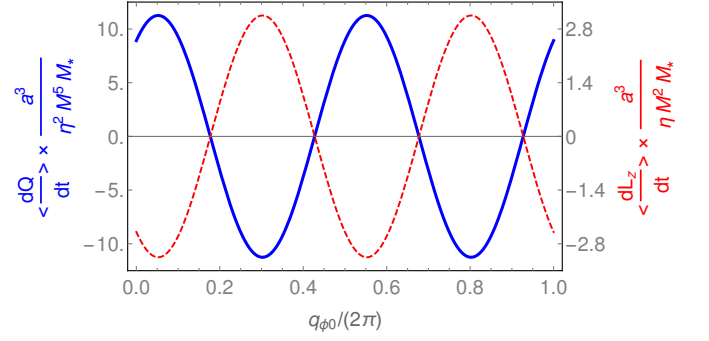


FIG. 1: Average change rate of the Carter constant (solid, blue) and angular momentum along the z -direction (dashed, red) as a function of $q_{\phi 0}$ for the case with $a = 0.99$ (see Tab. I). Both $\langle dQ/dt \rangle$ and $\langle dL_z/dt \rangle$ are normalized by ϵ to remove the associated linear dependence, and powers of M to be dimensionless.

assuming that the main evolution of the orbit is due to GW dissipation. Within this approximation [23, 24],

$$\left(\frac{\dot{J}_r}{\eta}, \frac{\dot{J}_\theta}{\eta}, \frac{\dot{J}_\phi}{\eta} \right) = - \sum_{lmkn} \frac{(n, k, m)}{2\omega_{mkn}^3} \left(|\tilde{Z}_{lmkn}^{\text{out}}|^2 + \alpha_{lmkn} |\tilde{Z}_{lmkn}^{\text{down}}|^2 \right), \quad (12)$$

where the coefficient α_{lmkn} , the asymptotic Teukolsky wave amplitude at infinity $\tilde{Z}_{lmkn}^{\text{out}}$ and at the horizon $\tilde{Z}_{lmkn}^{\text{down}}$ are defined in [25] [36]. For a given resonance, we compute the wave amplitudes and α_{lmkn} by solving the Teukolsky equation in the frequency domain, with a source term associated with the stellar-mass object's orbital motion at frequencies $(\omega_r, \omega_\theta, \omega_\phi)$. Our code agrees very well with other Teukolsky equation solvers [25].

For the $a = 0.99$ initial conditions, $T_{\text{res}} \sim (\eta\Gamma)^{-1/2} \sim 14\eta^{-1/2}M$ and the ratio between T_{res} and T_{td} is

$$\frac{T_{\text{res}}}{T_{\text{td}}} \sim 1.2 \left(\frac{\mu}{10M_\odot} \right)^{-\frac{1}{2}} \left(\frac{M}{M_{\text{SgrA}^*}} \right)^2 \left(\frac{R}{4.3 \text{ AU}} \right)^{-\frac{3}{2}}, \quad (13)$$

where μ is the mass of the small inspiraling body. These timescales are comparable for this example, so we are in the regime $T_{\text{res}} \sim T_{\text{td}}$ and must shift the resonance (including Ω_ϕ in the resonance condition), as compared to the static perturber approximation. Since $\Omega_\phi/\omega_\phi \sim 7.1 \times 10^{-3}(r/4M_{\text{SgrA}^*})^{3/2}(R/4.3 \text{ AU})^{-3/2}$, this shift is negligible in evaluating the resonance strength.

Impact on orbital phase. To estimate the effect of tidal resonances on the phase of GW waveforms, we evolve two orbits starting at the point of tidal resonance considered in Fig. 1, one with and one without ΔJ_i included. This evolution is realized with the orbit-averaged fluxes in Eq. (12) evaluated at each time step computed

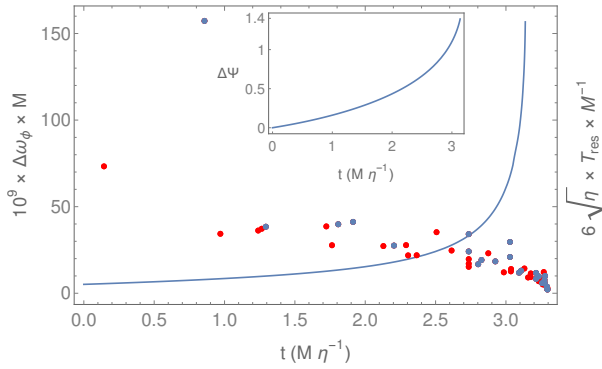


FIG. 2: Evolution of the difference in ω_ϕ between inspirals with and without resonant ΔJ_i (blue curve), and illustration of resonances encountered during inspiral (dots). We take the central black hole to have $M = M_{\text{SgrA}^*}$; both the inspiraling body μ and the perturbing tidal source M_* are $10 M_\odot$; and the tidal source is at separation $R = 4.3 \text{ AU}$. The orbits start at the resonance point $q_{\phi 0} = 0.33$ in Fig. 1; the final time is the plunge. Red and blue dots show the resonance duration T_{res} for resonances with $\{|m|, |k|, |n|\} \leq 5$; blue dots indicate $m = \pm 2$. (The right-hand vertical axis has the same scale as the left.) The tightly bunched dots in the lower right illustrate how the system passes rapidly through multiple tidal resonances in quick succession as plunge is approached. The inset shows the associated accumulated phase shift.

with the Teukolsky code, which in turn are used to update J_r, J_θ, J_ϕ and subsequently E, Q, L_z in time. At each time we compare ω_ϕ . Its difference is plotted in Fig. 2. To estimate the deviation in orbital phase caused by the tidal resonance, we evaluate (c.f. Fig. 2)

$$\begin{aligned} \Delta\Psi &:= \int_0^{T_{\text{plunge}}} 2\Delta\omega_\phi dt \\ &= 1.4 \left(\frac{\mu}{10M_\odot} \right)^{-\frac{1}{2}} \left(\frac{M}{M_{\text{SgrA}^*}} \right)^{\frac{7}{2}} \left(\frac{M_*}{10M_\odot} \right) \left(\frac{R}{4.3 \text{ AU}} \right)^{-3}, \end{aligned} \quad (14)$$

where T_{plunge} is the time of the plunge after the tidal resonance; in this example, $T_{\text{plunge}} \simeq 0.78(M/M_{\text{SgrA}^*})$ year. The factor of 2 in Eq. (14) is because the strongest GW harmonic is the $m = 2$ mode. For systems with $R \lesssim 4.3 \text{ AU}$ [as examined in Eq. (3)], the time till plunge is $\sim R^4$ [c.f. Eq. (1)]. As such, the fraction of the population undergoing tidal resonances scales as $(R/4.3 \text{ AU})^4$. However, it is important to note that the effect should be generally smaller for lighter massive BHs with less number of EMRI inspiral cycles.

To estimate the phase resolution of EMRI measurements, we adopt the Fisher-information analysis presented in [26, 27]. The statistical phase uncertainty roughly scales as $\sqrt{D} - 1/\text{SNR}$, where D is the number of intrinsic source parameters in the waveform, and SNR is the measured signal-to-noise ratio. By the Monte-Carlo study of [28], the number of EMRIs detected by LISA is

likely to be $\mathcal{O}(10) - \mathcal{O}(10^3)$ per year at an SNR detection threshold of 20. As SNR roughly scales as $1/d$ (with d distance to Earth) and the number of sources per unit distance scales as d^2 , we can estimate the average SNR of detected events to be ~ 30 . We thus roughly estimate the phase resolution to be $\Delta\Psi \sim 0.1$. This suggests that the phase shift estimated in Eq. (14) should be easily detectable. A significant fraction of EMRIs are likely to experience tidal resonances that induce $\Delta\Psi \geq 0.1$. Even if this holds for only 10% of EMRI events, this corresponds to $\mathcal{O}(1) - \mathcal{O}(100)$ events per year.

The above estimate is based on a particular resonance for a single EMRI orbit. A more rigorous calculation should survey a generic distribution of EMRI parameters and the mass/spin distribution of all host BHs. It will also be important to include the influence of other signals which are simultaneously “on” during LISA observation, such as massive black hole inspirals, close white dwarf binaries in our galaxies, and other EMRI events which are being observed contemporaneously. Most EMRI evolutions will cross multiple tidal resonances before plunge, as shown by the red dots in Fig. 2. At early times, there are several resonances with duration comparable to the initial resonance which may contribute a comparable phase shift. Many short-lived tidal resonances cluster before the plunge due to the EMRI’s rapidly changing orbital frequencies. Although their individual influence on the orbital phase is likely to be small compared to the initial resonance, there are many contributions. These late resonances may also overlap, yielding collective effects.

Discussion. Similar to the Newtonian Kozai-Lidov effect, close orbits in a Kerr spacetime satisfying Eq. (6) can be resonantly excited by an external tidal field, resulting in a secular shift in its orbital angular momentum [37]. EMRIs and tidal disruption events arise from the stellar clusters around massive BHs, and it has long been discussed that population studies of these events can be used to understand cluster properties and the growth history of massive black holes [2, 29–31]. Tidal resonance will enhance what is learned from EMRI events, providing additional data about other massive objects near galaxy centers, essentially probing the outliers of the stellar-mass distribution in these clusters. This information will come at the cost of a more complicated EMRI waveform model. Much effort is currently going into making accurate self-force-based EMRI models, iterating in perturbation theory to second order in the mass ratio, and including effects like the impact of the smaller body’s spin. Tidal resonances – if not carefully modeled for – may ultimately limit the precision to which it is worthwhile to make these waveform models. When testing General Relativity (GR) with EMRI observations in LISA, it is important not to miss attribute environmental effects as signals of GR violation.

The Mathematica notebooks used for these calcula-

tions, including the metric perturbation and computation of G_i , are available upon request.

Acknowledgements. H.Y. thanks Christopher Hirata for sharing his Teukolsky code, and Eric Poisson for valuable discussions and comments. B.B. thanks Nicolás Yunes for sharing his Maple notebook with the tidally perturbed metric. H.Y. acknowledges support from the Natural Sciences and Engineering Research Council of Canada. This research was supported in part by the Perimeter Institute for Theoretical Physics. Research at Perimeter Institute is supported in part by the Government of Canada through the Department of Innovation, Science and Economic Development Canada and by the Province of Ontario through the Ministry of Economic Development, Job Creation and Trade. S.A.H. is supported by NSF Grant PHY-1707549 and NASA Grant 80NSSC18K1091.

-
- [1] I. Martín-Navarro, J. P. Brodie, A. J. Romanowsky, T. Ruiz-Lara, and G. van de Ven, *Nature* **553** (2018).
 - [2] C. P. L. Berry, S. A. Hughes, C. F. Sopuerta, A. J. K. Chua, A. Heffernan, K. Holley-Bockelmann, D. P. Mihaylov, M. C. Miller, and A. Sesana, arXiv:1903.03686 (2019).
 - [3] S. Naoz, *Ann. Rev. Astron. Astrophys.* **54**, 441 (2016), 1601.07175.
 - [4] E. E. Flanagan and T. Hinderer, *Physical Review Letters* **109**, 071102 (2012).
 - [5] M. Morris, *Astrophys. J.* **408**, 496 (1993).
 - [6] J. Miralda-Escude and A. Gould, *The Astrophysical Journal* **545**, 847 (2000).
 - [7] C. J. Hailey, K. Mori, F. E. Bauer, M. E. Berkowitz, J. Hong, and B. J. Hord, *Nature* **556**, 70 (2018).
 - [8] H. Yang, B. Bonga, Z. Peng, , and G. Li (in preparation).
 - [9] R. Emami and A. Loeb, arXiv:1903.02578 (2019).
 - [10] R. Emami and A. Loeb, arXiv:1903.02579 (2019).
 - [11] P. Amaro-Seoane, P. Brem, J. Cuadra, and P. J. Armitage, *The Astrophysical Journal Letters* **744**, L20 (2011).
 - [12] S. Babak, J. Gair, A. Sesana, E. Barausse, C. F. Sopuerta, C. P. L. Berry, E. Berti, P. Amaro-Seoane, A. Petiteau, and A. Klein, *Phys. Rev. D* **95**, 103012 (2017).
 - [13] H. Yang and M. Casals, *Physical Review D* **96**, 083015 (2017).
 - [14] E. Poisson, A. Pound, and I. Vega, *Living Reviews in Relativity* **14**, 7 (2011).
 - [15] T. Hinderer and E. E. Flanagan, *Physical Review D* **78**, 064028 (2008).
 - [16] C. W. Misner, K. S. Thorne, J. A. Wheeler, and D. I. Kaiser, *Gravitation* (Princeton University Press, 2017).
 - [17] U. Ruangsri and S. A. Hughes, *Physical Review D* **89**, 084036 (2014).
 - [18] J. Brink, M. Geyer, and T. Hinderer, *Physical Review Letters* **114**, 081102 (2015).
 - [19] C. P. Berry, R. H. Cole, P. Cañizares, and J. R. Gair, *Physical Review D* **94**, 124042 (2016).
 - [20] S. A. Teukolsky, *Astrophys. J.* **185**, 635 (1973).
 - [21] N. Yunes and J. Gonzalez, *Phys. Rev. D* **73**, 024010 (2006).
 - [22] E. Poisson, *Phys. Rev. D* **70**, 084044 (2004).
 - [23] N. Sago, T. Tanaka, W. Hikida, and H. Nakano, *Progress of Theoretical Physics* **114**, 509 (2005).
 - [24] C. M. Hirata, *Physical Review D* **83**, 104024 (2011).
 - [25] S. Drasco and S. A. Hughes, *Physical Review D* **73**, 024027 (2006).
 - [26] L. Lindblom, B. J. Owen, and D. A. Brown, *Phys. Rev. D* **78**, 124020 (2008), 0809.3844.
 - [27] K. Chatziioannou, A. Klein, N. Yunes, and N. Cornish, *Physical Review D* **95**, 104004 (2017).
 - [28] J. R. Gair, S. Babak, A. Sesana, P. Amaro-Seoane, E. Barausse, C. P. Berry, E. Berti, and C. Sopuerta, in *Journal of Physics: Conference Series* (IOP Publishing, 2017), vol. 840, p. 012021.
 - [29] D. R. Pasham, D. Lin, R. Saxton, P. Jonker, E. Kara, N. Stone, P. Maksym, and K. Auchettl, arXiv:1903.02584 (2019).
 - [30] N. C. Stone and B. D. Metzger, *Monthly Notices of the Royal Astronomical Society* **455**, 859 (2015).
 - [31] P. Amaro-Seoane and M. Preto, *Classical and Quantum Gravity* **28**, 094017 (2011).
 - [32] E. Poisson, *Physical Review D* **91**, 044004 (2015).
 - [33] In general, the perturber's orbit should be eccentric. The tidal effect is larger when the perturber is close to the pericenter, and smaller when it is close to the apocenter. Multiple perturbers may contribute to the tidal environment. However, as the tidal strength sensitively depends on the distance, only closest BHs matter.
 - [34] There is an overall factor of two missing in $h_{\alpha\beta}$ in [21] as dL_z/dt at large radii yields half the Newtonian result. After correcting for this factor, $G_i^{(1)}$ agrees in the slow spin limit with $G_i^{(1)}$ for $h_{\alpha\beta}$ as in [32].
 - [35] The only non-zero resonances have $m = \pm 2$ given that the tidal perturber is on the equatorial plane so that $h_{\alpha\beta}$ only contains $m = \pm 2$ modes (in principle, the metric should also include $m = 0$ modes but those are not included in [21]). The $m : k : n = -2 : 1 : 2$ resonance vanishes because the tidal perturbation $h_{\alpha\beta}$ is reflection symmetric in the equatorial plane.
 - [36] The notation in [25] is slightly different from that used here: $\tilde{Z}_{lmkn}^{\text{out}}$ is denoted Z_{lmkn}^{H} in [25]; $\tilde{Z}_{lmkn}^{\text{down}}$ is denoted Z_{lmkn}^{∞} .
 - [37] The orbit of the third body is generally averaged over when performing the analysis of Newtonian Kozai-Lidov effect, in which case L_z of the inner orbit is also conserved, but the total angular momentum is not.